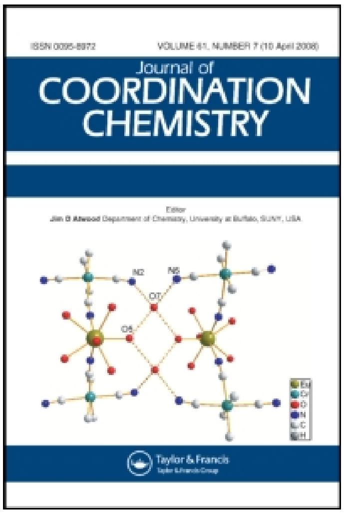

Journal of Coordination Chemistry
Publication details, including instructions for authors and subscription information:
http://www.informaworld.com/smpp/title~content=t713455674

Cadmium(II), manganese(II) and zinc(II) compounds

Rui-Feng Zhang[ab]; Wei Shi[a]; Hong-Sheng Wang[a]; Peng Cheng[a]
[a] Department of Chemistry, Nankai University, Tianjin 300071, China [b] Department of Chemistry, Shanxi Normal University, Shan Xi 041004, China

To cite this Article Zhang, Rui-Feng , Shi, Wei , Wang, Hong-Sheng and Cheng, Peng(2008) 'Cadmium(II), manganese(II) and zinc(II) compounds', Journal of Coordination Chemistry, 61: 10, 1606 — 1614
To link to this Article: DOI: 10.1080/00958970701609055
URL: http://dx.doi.org/10.1080/00958970701609055

Journal of Coordination Chemistry
Vol. 61, No. 10, 20 May 2008, 1606–1614

Taylor & Francis
Taylor & Francis Group

Cadmium(II), manganese(II) and zinc(II) compounds

RUI-FENG ZHANG*†‡, WEI SHI†,
HONG-SHENG WANG† and PENG CHENG†

†Department of Chemistry, Nankai University, Tianjin 300071, China
‡Department of Chemistry, Shanxi Normal University, Linfen,
Shan Xi 041004, China

(*Received 26 March 2007; in final form 24 May 2007*)

Three new compounds, $[Cd(\mu_3\text{-Hpdh})(\mu_2\text{-Cl})]_n$ (**1**), $Mn(Hpdh)_2(H_2O)_2$ (**2**) and $Zn(Hpdh)_2(H_2O)_2$ (**3**) (H_2pdh = pyridine-2,3-dicarbo-2,3-hydrazide), have been synthesized and characterized by elemental analysis, IR spectra, TG and single-crystal X-ray diffraction. Under hydrothermal conditions, H_2pdh is generated by an *in situ* acylation of H_2pda (H_2pda = pyridine-2,3-dicarboxylic acid) with hydrazine hydrate. Complex **1** features a 2D layer structure constructed by a dinuclear Cd(II) building block. In complexes **2** and **3**, hydrogen bonding interactions connect mononuclear structures into 3D supramolecular frameworks.

Keywords: Hydrothermal synthesis; Crystal structure; *In situ* ligand synthesis

1. Introduction

Many efforts in the field of metal-organic coordination networks have been motivated by their intriguing network topologies and potential functions as new classes of materials [1–8]. Multifunctional bridging ligands have been synthesized using the hydrothermal method; numerous complexes with intriguing structures and special properties [10–12] can be isolated by this powerful technique.

In situ ligand synthesis was first put forward by Champness and coworkers [13] and more than ten types of *in situ* ligand reactions have been enumerated, as reviewed by Zhang in 2005 [14]. Compared with conventional methods, *in situ* ligand synthesis provides a convenient approach to obtain novel compounds, which can be impossible to achieve by normal methods [15]. The current progress clearly demonstrates the important role of *in situ* metal/ligand reactions in crystal engineering of functional coordination compounds and one-pot synthesis of some unusual organic ligands [16]. Here we report *in situ* ligand syntheses and structures of three new coordination complexes, $[Cd(\mu_3\text{-Hpdh})(\mu_2\text{-Cl})]_n$ (**1**), $[Mn(H_2pdh)_2(H_2O)_2]Cl_2$ (**2**) and $[Zn(H_2pdh)_2(H_2O)_2]Cl_2$ (**3**), in which H_2pdh was prepared via *in situ* acylation of pyridine dicarboxylic acid and hydrazine hydrate.

---

*Corresponding author. Email: nkzrf@163.com

Journal of Coordination Chemistry
ISSN 0095-8972 print/ISSN 1029-0389 online © 2008 Taylor & Francis
DOI: 10.1080/00958970701609055

2. Experimental section

2.1. *Materials and methods*

All chemicals and solvents were of reagent grade and used without further purification. Elemental analyses for C, H and N were carried out on a Model 240 Perkin-Elmer elemental analyzer. The infrared spectrum was taken on a Bruker Tensor 27 Fourier transform infrared instrument in the 4000–400 cm^{-1} region using KBr pellets. The thermogravimetric analyses (TGA) for the three compounds were carried out on a NETZSCH TG 209 from room temperature to 800°C at a heating rate of 10°C min^{-1}. The photoluminescence spectrum was measured on a MPF-4 fluorescence spectrophotometer with a xenon arc lamp as the light source.

2.2. *Synthesis of [Cd(*μ_3*-Hpdh)(*μ_2*-Cl)]*$_n$ *(1)*

A mixture of $CdCl_2 \cdot 2.5H_2O$ (0.232 g, 1.02 mmol), H_2pda (0.176 g, 1.05 mmol), hydrazine hydrate (0.381 g, 7.61 mmol) and H_2O (5 mL, 277 mmol) was stirred at room temperature for 10 min and the pH was adjusted with dilute aqueous hydrochloric acid to 4 ~ 6. Then the mixture was sealed in a 30 mL Teflon-lined stainless steel autoclave (25 mL, capacity) under autogenous pressure, heated to 170°C for 3 days and cooled to room temperature. The crystalline product was filtered. Yellow single crystals suitable for X-ray analysis were obtained. Yield: 27%. Anal. Calcd for $C_7H_4CdClN_3O_2$: C 27.21, H 0.98, N 13.60%. Found: C 27.36, H 1.02, N 13.53%. IR (KBr cm^{-1}): 3191(m), 1636(s), 1572(s), 1531(s), 1369(m), 1250(m), 1221(m), 1115(m), 841(w), 793(m), 751(m), 666(w), 488(w).

2.3. *Synthesis of [Mn(Hpdh)*$_2$*(*H_2O*)*$_2$*] (2)*

The same synthesis procedure was employed except replacing $CdCl_2 \cdot 2.5H_2O$ with $MnCl_2 \cdot 6H_2O$. Yield: 37%. Anal. Calcd for $C_{14}H_{12}MnN_6O_6$: C 40.50, H 2.91, N 20.24%. Found: C 40.37, H 2.77, N 20.32%. IR (KBr cm^{-1}): 3064(m), 1637(s), 1482(s), 1395(s), 1350(s), 1218(s), 1115(s), 1094(m), 857(s), 794(s), 720(m), 655(m), 490(m), 434(m).

2.4. *Synthesis of [Zn(Hpdh)*$_2$*(*H_2O*)*$_2$*] (3)*

The reaction is analogous to that of **1**, except that $ZnCl_2 \cdot H_2O$ was used and pH value was adjusted to 2.0 with dilute hydrochloric acid. Yield: 42%. Anal. Calcd for $C_{14}H_{12}ZnN_6O_6$: C 39.32, H 3.30, N 19.65%. Found: C 39.41, H 3.22, N 19.52%. IR (KBr cm^{-1}): 3167(m), 1681(s), 1599(m), 1542(s), 11,468(s), 1395(m), 1338(m), 1206(m), 1114(m), 860(m), 778(s).

2.5. *X-ray crystallography*

Single crystals of **1**, **2** and **3** suitable for X-ray diffraction were glued to fine glass fibers and were then mounted on a Bruker SMART 1000 CCD diffractometer equipped with graphite-monochromated Mo-Kα radiation, $\lambda = 0.71073$ Å. The intensity data were collected at 294(2) K by using the ω-scan technique. Lorentz polarization and absorption corrections were applied. The structures were solved by direct methods and refined with the full-matrix least-squares technique using the SHELXS-97 and SHELXL-97 programs [17]. Anisotropic thermal parameters were assigned to all non-hydrogen atoms. The hydrogen atoms were set in calculated positions and refined as riding atoms with a common fixed isotropic thermal parameter. The crystallographic data and selected bond lengths and angles of **1**, **2** and **3** are listed in tables 1 and 2, respectively.

3. Results and discussion

3.1. *Synthesis of the complexes*

Coordination compounds are commonly obtained by reaction of commercially available or pre-synthesized ligands. For *in situ* ligand synthesis, ligand precursors are directly used to react with metal ions simplifying synthetic steps and providing a more convenient and environmentally-friendly way to obtain complexes. The acylation reaction of H_2pda took place during the formation of **1**, **2** and **3**, as shown in scheme 1.

Table 1. Crystallographic data and structural refinement for **1**–**3**.

	1	**2**	**3**
Empirical formula	$C_7H_3CdClN_3O_2$	$C_{14}H_{12}MnN_6O_6$	$C_{14}H_{14}ZnN_6O_6$
Formula weight	308.97	415.24	427.68
Crystal system	Monoclinic	Triclinic	Monoclinic
Space group	$P2(1)/c$	$P\bar{1}$	$P2(1)/c$
Unit cell dimensions (Å, °)			
a	7.2901(9)	5.1974(14)	12.724(2)
b	10.6226(14)	8.634(2)	95.674(4)
c	10.9652(14)	9.548(3)	104.207(4)
α	90	102.563(4)	90
β	107.666(2)	95.674(4)	100.511(3)
γ	90	104.207(4)	90
Volume (Å^3)	809.10(18)	400.17(18)	725.7(2)
$F(000)$	588	211	436
Z, D_{Calcd} (g cm^{-3})	4, 2.536	1, 1.723	2, 1.748
Goodness-of-fit on F^2	1.083	1.095	1.172
Absorption coefficient (mm^{-1})	2.998	0.875	1.748
Crystal size (mm^3)	$0.20 \times 0.16 \times 0.14$	$0.38 \times 0.22 \times 0.12$	$0.22 \times 0.12 \times 0.08$
θ range (°)	2.73–27.17	2.21–26.31	3.83–25.01
Index ranges	$-5 \le h \le 9$	$-4 \le h \le 6$	$-14 \le h \le 15$
	$-13 \le k \le 13$	$-10 \le k \le 10$	$-6 \le k \le 3$
	$-13 \le l \le 14$	$-10 \le l \le 11$	$-12 \le l \le 12$
Data/restraints/parameters	1783/0/127	1607/0/136	1279/3/132
Reflections collected	4599	2245	3501
Independent reflections	1783 ($R_{int} = 0.0159$)	1607 ($R_{int} = 0.0159$)	1279 ($R_{int} = 0.0159$)
Largest diff. peak and hole (e A^{-3})	0.635 and -0.481	0.283 and -0.238	0.287 and -0.722
Final R indices ($I > 2\sigma(I)$)	$R_1 = 0.0198$,	$R_1 = 0.0288$,	$R_1 = 0.0274$,
	$wR = 0.0510$	$wR = 0.0770$	$wR = 0.0783$,
R indices (all data)	$R_1 = 0.0225$,	$R_1 = 0.0329$,	$R_1 = 0.0352$,
	$wR = 0.0522$	$wR = 0.0792$	$wR = 0.0844$

Table 2. Selected bond lengths (Å) and angles (°) for **1**–**3**.

1					
Cd(1)–N(2B)	2.318(2)	Cd(1)–O(2D)	2.416(2)	O(2E)–Cd(1A)	2.416(2)
Cd(1)–O(1)	2.3388(19)	Cd(1)–Cl(1)	2.572(7)	N(2C)–Cd(1A)	2.318(2)
Cd(1)–N(1)	2.364(2)	Cd(1)–Cl(1A)	2.6240(8)	Cl(1)–Cd(1A)	2.6240(8)
N(2B)–Cd(1)–O(1)	172.91(7)	O(1)–Cd(1)–N(1)	71.83(7)	O(1)–Cd(1)–O(2D)	86.50(7)
N(2B)–Cd(1)–N(1)	108.81(7)	N(2B)–Cd(1)–O(2D)	86.48(7)	N(1)–Cd(1)–O(2D)	87.77(7)
N(2B)–Cd(1)–Cl(1)	89.18(6)	N(1)–Cd(1)–Cl(1)	161.68(5)	O(1)–Cd(1)–Cl(1)	89.89(5)
O(2D)–Cd(1)–Cl(1)	90.01(5)	N(2B)–Cd(1)–Cl(1)A	99.28(6)	O(1)–Cd(1)–Cl(1A)	87.71(5)
N(1)–Cd(1)–Cl(1A)	92.60(6)	O(2D)–Cd(1)–Cl(1A)	173.77(5)	Cl(1)–Cd(1)–Cl(1A)	87.69(2)
Cd(1)–Cl(1)–Cd(1A)	92.31(2)	C(6)–O(1)–Cd(1)	114.07(16)	C(5)–O(2)–Cd(1A)	119.41(17)
2					
C(1)–N(1)–Cd(1)	129.37(18)	C(7)–N(1)–Cd(1)	112.12(16)	N(3B)–N(2B)–Cd(1A)	116.62(15)
C(6)–N(2)–Cd(1A)	123.45(16)				
Mn(1)–O(1A)	2.1091(12)	Mn(1)–O(3)	2.2718(15)	Mn(1)–N(1)	2.2748(14)
Mn(1)–O(1)	2.1091(12)	Mn(1)–O(3A)	2.2717(15)	Mn(1)–N(1A)	2.2748(14)
3					
O(1A)–Mn(1)–O(1)	180.0	O(3)–Mn(1)–O(3A)	180.0	O(1)–Mn(1)–O(3A)	89.18(6)
O(1A)–Mn(1)–O(3)	89.18(6)	O(1A)–Mn(1)–N(1)	102.79(5)	O(3)–Mn(1)–N(1A)	88.95(5)
O(1)–Mn(1)–O(3)	90.82(6)	O(1)–Mn(1)–N(1)	77.21(5)	O(3A)–Mn(1)–N(1A)	91.05(5)
O(1)–Mn(1)–O(3A)	90.82(6)	O(1)–Mn(1)–N(1A)	102.79(5)	N(1)–Mn(1)–N(1A)	180.00(4)
Zn(1)–N(1A)	2.086(2)	Zn(1)–O(1)	2.0868(19)	Zn(1)–O(3A)	2.169(2)
Zn(1)–N(1)	2.086(2)	Zn(1)–O(1A)	2.0868(19)	Zn(1)–O(3)	2.169(2)
N(1A)–Zn(1)–N(1)	180.000(1)	O(1)–Zn(1)–O(1A)	180.0	N(1A)–Zn(1)–O(3)	89.25(9)
N(1A)–Zn(1)–O(1)	98.93(8)	N(1A)–Zn(1)–O(3A)	90.75(9)	N(1)–Zn(1)–O(3)	90.75(9)
N(1)–Zn(1)–O(1)	81.07(8)	N(1)–Zn(1)–O(3A)	89.25(9)	O(1)–Zn(1)–O(3)	90.01(9)
N(1A)–Zn(1)–O(1A)	81.07(8)	O(1)–Zn(1)–O(3A)	89.99(9)	O(1A)–Zn(1)–O(3)	89.99(9)
N(1)–Zn(1)–O(1A)	98.93(8)	O(1A)–Zn(1)–O(3A)	90.01(9)	O(3A)–Zn(1)–O(3)	179.999(1)

Symmetry code: (**1**) A: $-x+2,\ y+1/2,\ -z+1/2$, B: $-x+2,\ -y,\ -z$, C: $-x+2,\ -y,\ -z+1$, D: $-x+2,\ y-1/2,\ -z+1/2$; (**2**) A: $-x+1,\ -y,\ -z+1$; (**3**) A: $-x+2,\ -y+2,\ -z+2$.

$n\mathrm{CdCl_2{\cdot}2.5H_2O} + n\mathrm{H_2pda} + n\mathrm{N_2H_4{\cdot}H_2O} \xrightarrow[\mathrm{H_2O}]{170^\circ\mathrm{C}}$ $[\mathrm{Cd}(\mu_3\text{-Hpdh})(\mu_2\text{-Cl})]_n$ (**1**) + other products

$\mathrm{MnCl_2{\cdot}6H_2O} + 2\mathrm{H_2pda} + 2\mathrm{N_2H_4{\cdot}H_2O} \xrightarrow[\mathrm{H_2O}]{170^\circ\mathrm{C}}$ $[\mathrm{Mn(Hpdh)_2(H_2O)_2}]$ (**2**) + other products

$\mathrm{ZnCl_2{\cdot}H_2O} + 2\mathrm{H_2pda} + 2\mathrm{N_2H_4{\cdot}H_2O} \xrightarrow[\mathrm{H_2O}]{170^\circ\mathrm{C}}$ $[\mathrm{Zn(Hpdh)_2(H_2O)_2}]$ (**2**) + other products

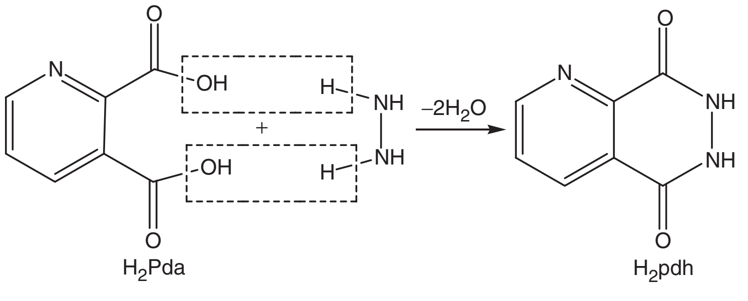

Scheme 1. Formation of the ligand.

3.2. *Description of the crystal structure of (1)*

Complex **1** is composed of a dinuclear Cd(II) secondary building unit (SBU). As illustrated in figure 1(a), Cd(II) is in an octahedral environment and coordinated by two μ_2-Cl [Cd(1)–Cl(1) 2.572(7) Å, Cd(1)–Cl(1A) 2.6240(8) Å], two $O_{carbonyl}$ atoms [Cd(1)–O(1) 2.3388(19) Å, Cd(1)–O(2D) 2.416(2) Å] and two nitrogen atoms [Cd(1)–N(1) 2.364(2) Å, Cd(1)–N(2B) 2.318(2) Å]. Hpdh is a μ_3-bridge to connect such SBUs into a 2D layer structure (figure 1b). The π–π interaction is important in forming the 3-D structures from 2-D layers. The dihedral angle between adjacent pyridine rings is 0° and the distance between the pyridine ring planes from adjacent layers is rather short, with centroid separation 3.506(2) Å, interplaner spacing 3.3919 Å (average 3.3–3.8 Å), implying that strong π–π interactions exist in **1**. In addition, there are extensive C–H↑O hydrogen-bonding interactions involving carbonyl oxygen atoms and carbon atoms of pyridine rings; the distance between C and O is 3.331 Å and the bond angle is 159.4°.

3.3. *Description of the crystal structure of (2)*

The structure of **2** is a discrete neutral molecule, as shown in figure 2(a). Mn(II) is coordinated by two oxygen atoms and two nitrogen atoms from two deprotonated H_2pdh ligands at the basal plane [Mn(1)–O(1) 2.1091(12) Å, Mn(1)–N(1) 2.2748(14) Å] and two aqua molecules at the apical positions [Mn(1)–O(3) 2.2718(15) Å] to complete octahedral geometry. Hydrogen bonding plays an important role in constructing

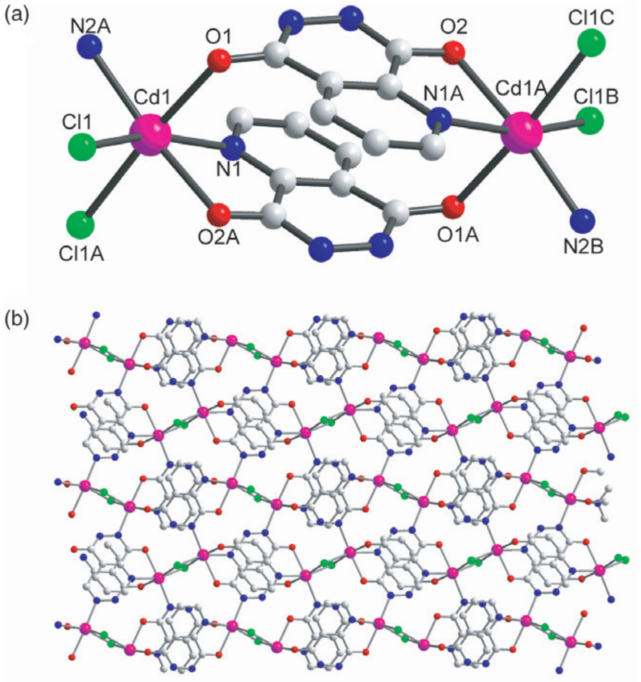

Figure 1. View of dinuclear building block for (a) and two-dimensional layer structure of **1** for (b). Purple, Cd; gray, C; blue, N; red, O; green, Cl.

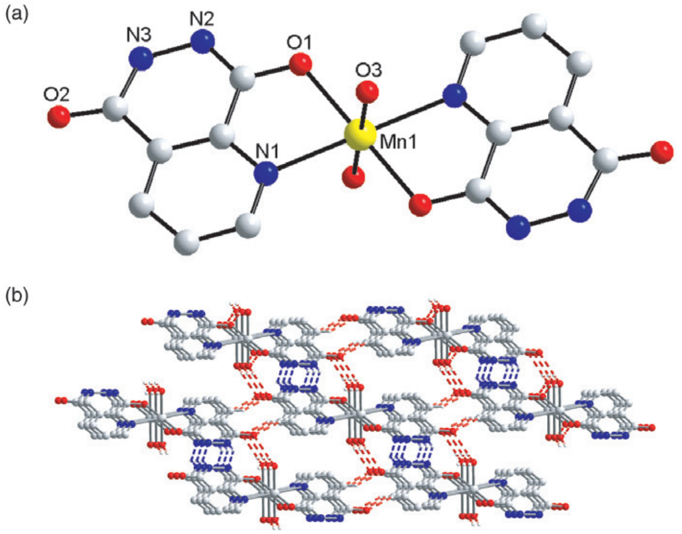

Figure 2. Mononuclear structure for (a) and 3D supramolecular framework of **2** for (b). Yellow, Mn; gray, C; blue, N; red, O; black line, coordination bond; red dotted line, C–H↑O hydrogen bond; blue dotted line, N–H↑N hydrogen bond.

the 3D network of **2**. As shown in figure 2(b), adjacent molecules are linked through N–H↑N (2.01 Å) and C–H↑O (2.29 Å) hydrogen bonds to form a 2D plane. Furthermore, O–H↑O (1.95 Å) hydrogen bonds between aqua oxygen atoms and carbonyl oxygen atoms connect 2D planes into a 3D framework. Although the pyridine planes of adjacent layers parallel each other, no π–π interactions exist because the centroid–centroid distance is 4.2 Å, much larger than the average value 3.3–3.8 Å [16].

3.4. *Description of the crystal structure of (3)*

The structure of **3** also shows a mononuclear structure, as indicated in figure 3(a). The dihedral angle between adjacent pyridine planes is 75.8° and the coordination environment of Zn(II) is the same as Mn(II) in **2**, while their 3D frameworks are quite different (figure 3b). N–H↑O (2.04 Å) and O–H↑O (2.50 Å) hydrogen bonds link the neighboring molecules into a 1D chain. But the molecules are not parallel and are linked through O–H↑O hydrogen bonds into a 3D network.

3.5. *Thermogravimetric analysis*

Thermal behaviors of the title complexes were observed from 20 to 800°C and the thermogravimetric curves of **1**, **2** and **3** are shown in figure 4. None underwent mass change below 100°C, implying that no crystalline water molecules exist. The framework of **1** is not broken until 285°C. Mass changes of 8.61 and 8.56% corresponding to coordinated water molecules in **2** and **3**, respectively, have been observed at 200°C. Above 400°C, complete decomposition of all the complexes is observed.

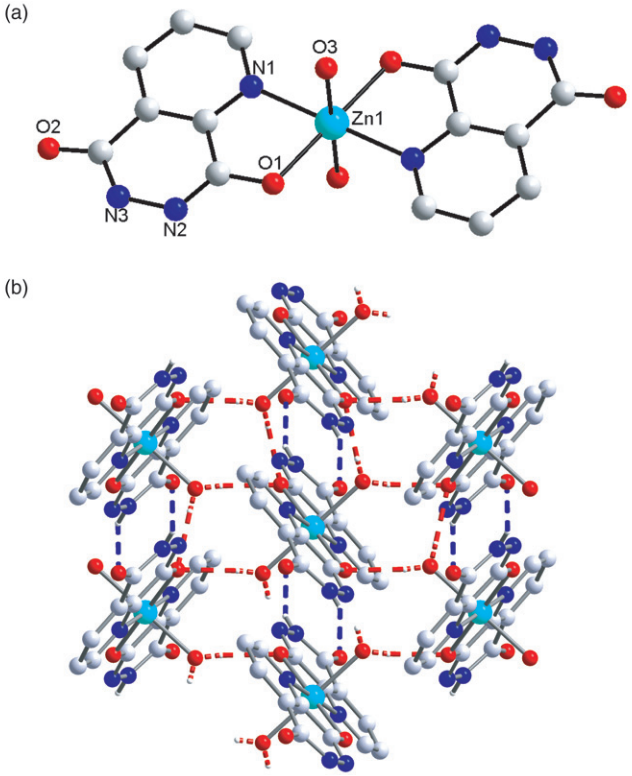

Figure 3. Mononuclear structure for (a) and 3D supramolecular framework of **3** for (b). Turquoise, Zn; gray, C; blue, N; red, O; black line, coordination bond; red dotted line, C–H↑O hydrogen bond; blue dotted line, N–H↑N hydrogen bond.

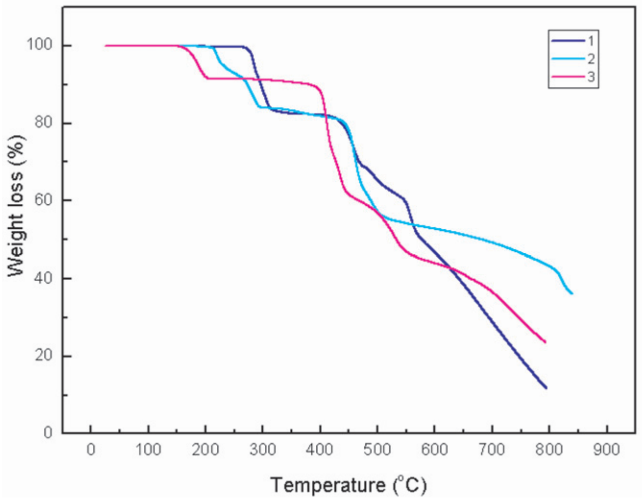

Figure 4. TG curves of **1**, **2** and **3**.

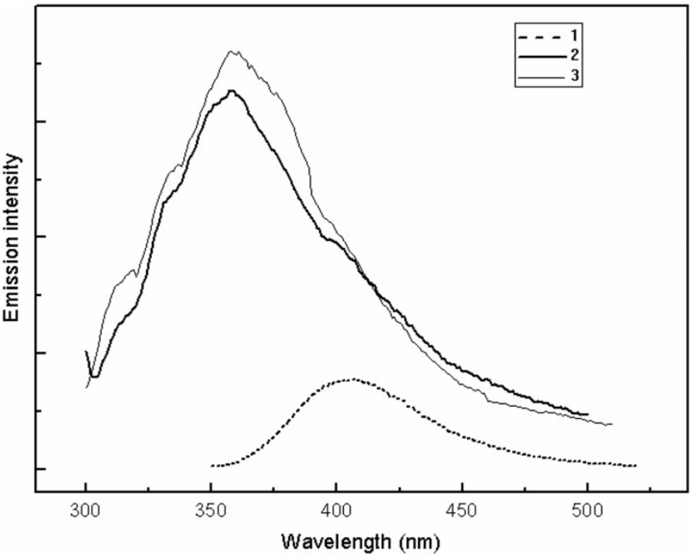

Figure 5. Emission spectra of H_2pda, compounds **1** and **3** (curve 1 for H_2pda, curve 2 for compound **1** and curve 3 for compound **3**).

3.6. *Photoluminescent properties*

The ability of metal complexes to enhance, shift and quench luminescent emission of organic ligands makes them promising materials for potential applications as light-emitting materials [18]. The solid-state emission spectra of H_2pda and **1** and **3** are shown in figure 5. A comparison of the fluorescence spectra of the ligand H_2pda and its metal complexes **1** and **3** is helpful for the emission origin. Free H_2pda exhibits an emission maximum at 407 nm when excited at 307 nm, while for **1** and **3** strong emissions at 358 and 357 nm are observed upon excitation at 278 and 286 nm, respectively. Complexes **1** and **3** showed highly enhanced fluorescence intensity compared with H_2pda. We tentatively attributed this to two reasons. First, the nitrogen atoms from hydrazine hydrate are strong electron donors which enhance the $\pi^* \to n$ transition of H_2pda. Second, the coordinated Zn and Cd atoms also play important roles in the significant blue-shift and emission enhancement of H_2pdh by effectively increasing the rigidity of the ligands and reducing the radiationless decay of the intraligand emission excited state [19]. It is obvious that **1** and **3** possess strong fluorescence intensity, which indicates potential application in solvent-resistant fluorescent materials due to their poor solubility in common solvents.

4. Conclusion

In summary, three new compounds have been prepared employing the *in situ* ligand synthetic method. Complex **1** is a 2D layer while **2** and **3** feature mononuclear structures and hydrogen bonds extend such monomeric units into 3D supramolecular frameworks. Both **1** and **3** exhibit strong fluorescence emission at 357 nm upon excitation at 278 and 286 nm, respectively. This method can be widely used to synthesize coordination complexes based on various *ortho*-dicarboxylic acids, hydrazine hydrate and transition metal ions.

Supplementary material

Crystallographic data for the structural analysis of **1**, **2** and **3** have been deposited with the Cambridge Crystallographic Data Center, CCDC: −282,873, −2,294,654, −2,94,655 for **1**, **2** and **3**, respectively. Copies of the data can be obtained free of charge from The Director, CCDC, 12 Union Road, Cambridge, CB2 1EZ, UK (Fax: +441223 336 033; email: deposit@ccdc.cam.ac.uk).

Acknowledgements

This work was supported by the National Natural Science Foundation of China (Nos 20631030 and 20425103), the NSF of Tianjin (No. 06YFJZJC009000), the State Key Project of Fundamental Research of MOST (2005CCA01200), and MOE (Grant 20060055039) of China.

References

[1] B. Moulton, M.J. Zaworotko. *Chem. Rev.*, **101**, 1029 (2001).
[2] O.R. Evens, W.B. Lin. *Acc. Chem. Res.*, **35**, 511 (2002).
[3] S. Kitagawa, R. Kitaura, S. Noro. *Angew. Chem. Int. Ed.*, **43**, 2334 (2004).
[4] N.C. Gianneschi, P.A. Bertin, S.T. Nguyen, C.A. Mirkin, L.N. Zaknarov, A.L. Rheingold. *J. Amer. Chem. Soc.*, **125**, 10508 (2003).
[5] J.W. Lee, S. Samal, N. Selvapalam, H.J. Kim, K. Kim. *Acc. Chem. Res.*, **36**, 621 (2003).
[6] F.M. Tabellion, S.R. Seidel, P.J. Arif, P.J. Stang. *Angew. Chem. Int. Ed.*, **40**, 1529 (2001).
[7] C. Janiak. *Dalton Trans.*, 2781 (2003).
[8] S.L. James. *Chem. Soc. Rev.*, **32**, 276 (2003).
[9] X.X. Hu, C.L. Pan, X.B. Cui, G.D. Yang, T.G. Wang. *Eur. J. Inorg. Chem.*, 1566 (2004).
[10] F.C. Liu, L.Y. Duan, Y.G. Li, E.B. Wang, X.L. Wang, C.W. Hu, L. Xu. *Inorg. Chim. Acta*, **357**, 1355 (2004).
[11] X.M. Zhang. *Eur. J. Inorg. Chem.*, 544 (2004).
[12] J. Blake, N.R. Champness, S.S.M. Chung, W.S. Li, M. Schröder. *Chem. Commun.*, 1675 (1997).
[13] X.M. Zhang. *Coord. Chem. Rev.*, **249**, 1201 (2005).
[14] D. Li, T. Wu. *Inorg. Chem*, **44**, 1175 (2005).
[15] C. Janiak. *J. Chem. Soc., Dalton Trans.*, 3885 (2000).
[16] X.M. Chen, M.L. Tong. *Acc. Chem. Res.*, **40**, 162 (2007).
[17] G.M. Sheldrick. SHELXTL V5.1 Software Reference Manual, Bruker AXS, Inc., Madison, Wisconsin, USA (1997).
[18] R.L. Sang, L. Xu. *Inorg. Chem.*, **44**, 3731 (2005).
[19] (a) L.Y. Zhang, G.F. Liu, S.L. Zheng, X.M. Chen, *et al. Eur. J. Inorg. Chem.*, 2965 (2003); (b) M. Prabhakar, P.S. Zacharias, S.K. Das. *Inorg. Chem.*, **44**, 2585 (2005).